fractal and fractional

MDPI

Article

Fractal Properties of Composite-Modified Carbon Paste Electrodes—A Comparison between SEM and CV Fractal Analysis

Gianina Dobrescu [1], Ramona Georgescu-State [2], Florica Papa [1], Jacobus (Koos) Frederick van Staden [2] and Razvan Nicolae State [1,*]

[1] "Ilie Murgulescu" Institute of Physical Chemistry of the Romanian Academy, 202 Splaiul Independentei Street, 060021 Bucharest, Romania; dobrescugianina@yahoo.com (G.D.); frusu@icf.ro (F.P.)
[2] Laboratory of Electrochemistry and PATLAB, National Institute of Research and Development for Electrochemistry and Condensed Matter, 202 Splaiul Independentei Street, 060021 Bucharest, Romania; state_ramona@yahoo.ro (R.G.-S.); koosvanstaden2012@yahoo.com (J.F.v.S.)
* Correspondence: rstate@icf.ro

Abstract: The fractal properties of carbon paste electrodes (CPEs) and carbon paste electrodes modified with ionic liquid (IL), $AuTiO_2$/graphene oxide, and IL/$AuTiO_2$/graphene oxide were investigated using scanning electron microscopy (SEM), and cyclic voltammetry (CV). The impact of fractal dimensions and self-similarity ranges on electrochemical responses was underlined. It was proved that a higher fractal dimension and a broad self-similarity domain lead to a higher electrochemical response. Results indicated that IL/$AuTiO_2$/graphene oxide composite-modified CPEs are a great candidate to be used as electrochemical sensors, with a high fractal dimension and large self-similarity domain.

Keywords: fractal dimension; SEM; CV; gold nanoparticles; carbon paste electrode

check for updates

Citation: Dobrescu, G.; Georgescu-State, R.; Papa, F.; Staden, J.F.v.; State, R.N. Fractal Properties of Composite-Modified Carbon Paste Electrodes—A Comparison between SEM and CV Fractal Analysis. *Fractal Fract.* **2024**, *8*, 205. https://doi.org/10.3390/fractalfract8040205

Academic Editor: Carlo Cattani

Received: 26 February 2024
Revised: 27 March 2024
Accepted: 29 March 2024
Published: 31 March 2024

Copyright: © 2024 by the authors. Licensee MDPI, Basel, Switzerland. This article is an open access article distributed under the terms and conditions of the Creative Commons Attribution (CC BY) license (https://creativecommons.org/licenses/by/4.0/).

1. Introduction

The IL/$AuTiO_2$/graphene oxide (GO) composite-modified carbon paste electrode was recently proven to be a successful sensor showing high selectivity, sensitivity, reproducibility, and good stability for the detection of tartrazine (Tz, E102) [1], a synthetic organic food dye that must be controlled due to its potential harmfulness to human health [2,3].

Low background current, fast regenerative surface, easy modification, and low cost make carbon paste electrodes (CPEs) the preferred electrode materials often used in electrochemistry [4,5].

In previous work [1], the carbon paste electrode was modified using an ionic liquid (IL) and $AuTiO_2$/GO composite to obtain a proper Tz sensor.

Since the first studies on fractal objects [6], there have been many reports in the literature showing the fractal nature of surfaces [7]. Moreover, the link between fractal properties and their physical–chemical properties has often been depicted in the last years: the fractal properties of the catalysts [8–11], zeolites [12], electrodes in electrochemical applications [13–19], nanoparticles [20,21], dental surfaces [22] have been intensively studied. Understanding the impact of roughness on surface phenomena and, moreover, the fact that most surfaces are self-affine (self-similar and scaling with different amounts in different directions) opened a new chapter in the study of adsorption [10], catalysis [8–11], and electrochemical processes [14,15,17–19,23,24].

The assumption that the electrode surface is Euclidean (planar, cylindrical, or spherical electrodes) leads to power laws, such as Cottrell, Sand, or Randles–Sevcik equations, used to analyze diffusion/transport phenomena in electrochemistry. However, experiments use surfaces that are not smooth or planar but rough. Moreover, as Mandelbrot [6] and later Avnir and Farin proved [7], surfaces are not only rough but are self-similar.

In the last years, applications of fractal theory in electrochemistry have constantly grown, including diffusion kinetics at the fractal electrodes, electrochemical responses to various signals under diffusion—limited reactions of fractal interfaces; the property of a fractal to minimize internal resistance while maximizing surface-to-volume ratios lead to better carbon electrodes [13] and the application of noise analysis and fractal geometry in understanding the corrosion mechanism of stainless steel immersed in different concentrations of $FeCl_3$ leads to fractal surfaces with good correlation between the surface fractal dimension obtained by electrochemical impedance spectroscopy and by scanning electron microscopy [16].

Fractal analysis is a powerful technique to investigate electrode surfaces [17,18]; it was also used in fractal dimension determination of dental surfaces as a quantitative measure of the state of the carious tooth surface [22]. Even energy efficient microelectrodes used in neurostimulation are affected by the fractal design, as studies showed superior properties of the fractal shape microelectrodes [13].

Self-similarity is the property of an object to look the same at different scales; fractal objects are self-similar, and they are characterized by a number, the fractal dimension, describing the fractal behavior on the self-similarity domain [6]. Surfaces are characterized by the surface fractal dimension related to both self-similarity and roughness.

To analyze surfaces as fractal objects it is necessary to compute their fractal dimensions. There are a lot of methods to do this, based on different experimental techniques of characterization, including microscopy (atomic force microscopy, scanning electron microscopy, transmission electron microscopy) [9,25], small angle X-ray scattering [26–29], cyclic voltammetry and electrochemical impedance spectroscopy [19], and adsorption [30–33].

In this work, carbon paste electrodes, IL-modified carbon paste electrodes, and $AuTiO_2$/GO and IL/$AuTiO_2$/GO composite-modified carbon paste electrodes were studied from a fractal behavior point of view.

Fractal dimensions were computed by SEM micrograph analysis (SEM fractal dimension) and by cyclic voltammetry (CV-fractal dimension).

The aim of this paper is to correlate the fractal properties of four types of electrodes: carbon paste electrodes, IL-modified carbon paste electrodes, $AuTiO_2$/GO and IL/$AuTiO_2$/GO composite-modified carbon paste electrodes with the electrochemical response and with the ability of the electrode to act as a sensor.

As a novelty, we shall demonstrate the following:

- The analyzed carbon paste electrodes are fractals with broad self-similarity domains; the modifications of carbon paste electrodes influence their fractal properties toward higher fractal dimensions and large self-similarity domains.
- An electrode with a higher fractal dimension leads to a better electrochemical response and, therefore, is suitable to be used as a Tz-sensor [1].
- A larger self-similarity domain will lead to a higher active area and a higher electrochemical response.
- Although the fractal dimensions obtained from cyclic voltammetry differ from those obtained from SEM images, there are correlations between them; SEM analysis offers information about the self-similarity domain.
- Conclusions on how the electrochemical response can be improved are also depicted.

The paper is structured in four sections. After Section 1 Introduction, Section 2 presents the theoretical and experimental methods. A brief exposition of the carbon paste electrode preparation is followed by a description of the experimental materials and apparatus used for characterization. The methods used to compute fractal dimensions are presented in Section 2.2. Results and discussions are in extenso presented in Section 3, followed by the major conclusions in Section 4.

2. Theoretical Methods and Experimental

2.1. Materials and Characterization

2.1.1. Preparation

Au nanoparticles (AuNPs) were prepared using a modified synthesis alkaline polyol method described in detail elsewhere [34]. The synthesized nanoparticles capped by PVP have a uniform structure, very good dispersion, and sizes between 6 nm and 16 nm, as depicted in a previous work [1].

$AuTiO_2$/GO composite was synthesized using 50 mg graphene oxide and 50 mg TiO_2, dispersed in ionized water and ultrasound, as Refs. [1,34] described. AuNPs were impregnated on the TiO_2/GO powder, resulting in a 5% metal load composite material.

The ionic liquid (1-butyl-2,3-dimethylimidazolium tetrafluoroborate) was added to carbon paste to form the modified carbon paste electrode, as in Ref. [1]. The utilization of TiO_2 and AuNPs improved the conductivity of the sensor, while the ionic liquid (IL) was used as an electrocatalyst.

2.1.2. Characterization

Fractal dimensions of the electrodes were computed based on two different methods: scanning electron microscopy (SEM) and cyclic voltammetry (CV).

To obtain SEM images, an FEI Company's Quanta Inspect F microscope with a field emission electron beam gun (FEG) and a resolution of 1.2 nm was used.

A mini potentiostat EmSTAT Pico connected to a laptop for data acquisition was used to obtain cyclic voltammograms. The electrochemical experiments were carried out at 22° C. The electrochemical cell contained three electrodes: the modified carbon paste electrode as the working electrode, Ag/AgCl as the reference electrode, and Pt-wire as the auxiliary electrode. Apparatus and methods were described in detail in a previous paper [1].

2.2. Fractal Theory and Methods

2.2.1. Fractal Dimension Computation by SEM Method

The surface morphology of the sensors was depicted using the SEM technique. The presence of Au/TiO_2 and $AuTiO_2$/GO composite was proven from the EDAX spectrum and SEM mapping. Results were presented in a previously published paper [1]. Various methods can be used to compute the fractal dimension from SEM micrograph analysis, such as the power spectral density (PSD) method using Fourier transform function [35], the box-counting method [6], the mass-radius relation method [36], the correlation function method [36,37], and the variable length scale method [38]. We used the correlation function method [37] and the variable length scale method [38] to compute fractal dimension from SEM micrograph analysis.

To characterize the fractal behavior of the surface, both the fractal dimension and the self-similarity inner and outer cut-offs must be computed. The self-similarity cut-offs describe the limits between fractal properties that are valid.

The correlation function method uses the height correlation function, which scales in space; the slope of the log-log plot of the correlation function versus correlation distance is 2(3-D), where D is the fractal dimension [37] as in the following:

$$G(r) \equiv < \left[h\left(\vec{x}\right) - h\left(\vec{x} + \vec{r}\right) \right]^2 >_x \quad (1)$$

where the symbol <. . .> denotes an average over x, and the scaling law is:

$$G(r) \sim r^{2(3-D)}, r << L \quad (2)$$

On the other hand, the variable length scale method uses the surface roughness, averaged over each box of linear size ε, which is a power function of ε with exponent (3-D), with D the fractal dimension [38]. The log-log plot of the averaged surface roughness versus the box size leads to (3-D).

Rms deviation $R_{q\varepsilon}$, averaged over n_ε, the number of intervals of length ε, is defined by:

$$R_{q\varepsilon} = \frac{1}{n_\varepsilon}\sum_{i=1}^{n_\varepsilon}\sqrt{\frac{1}{p_\varepsilon}\sum_{j=1}^{p_\varepsilon} z_j^2} \tag{3}$$

where z_j is the jth height variation from the best-fit line within the interval i, and p_ε is the number of points in the interval ε.

The log-log plot of $R_{q\varepsilon}$ versus ε gives the Hurst or roughening exponent H, and the fractal dimension D can be calculated as:

$$D = D_T - H \tag{4}$$

where D_T is the topological dimension of the embedding Euclidean space (D_T = 2 for profiles and D_T = 3 for surfaces).

As a remark, the correlation function method gives better results at lower scale values; meanwhile, the variable scaling method works better at large scales, computing global fractal dimensions.

Fractal dimensions obtained using both the correlation function method and variable length scale method measure the self-affinity of the surface and, therefore, take values between 2 and 3. For a higher roughness, the fractal dimension will be close to 3; meanwhile, a surface with lower roughness will be characterized by a fractal dimension close to 2 (planar surface).

SEM micrographs are converted into 3-dimensional images where the grey level of each (x,y) pixel is assigned to the surface height at the (x,y) surface coordinates. Both the height correlation function method and the variable length scale method were computed using an implemented C++ computer code.

2.2.2. Fractal Dimension Computation Using the Cyclic Voltammetry (CV) Method

The voltammetric response of fractal surfaces was intensively studied. There are two methods to compute fractal dimension from CV investigation. The first one is based on the remark that the potential separation between anodic and cathodic peaks is a function of the fractal dimension [19], and the second one is based on the Randles–Sevcik equation [19], which offers, in a log-log plot, the fractal dimension as the slope of the curve.

In this work, to compute the fractal dimension, the fractal Randles–Sevcik equation was used [19]:

$$i_{peak} = \frac{\Gamma(1-\alpha)\Gamma(\alpha)\left(\gamma\lambda_i^2\right)^{\alpha-\frac{1}{2}}(nFv)^\alpha nFA_{macro}D^{1-\alpha}C_o^*\chi_{\max(\alpha)}}{\Gamma\left(\frac{1}{2}\right)(RT)^\alpha} \tag{5}$$

where $\alpha = (D-1)/2$, with α being the well-known fractal parameter of diffusion on a fractal surface and D being the CV-fractal dimension; A_{macro} is the macroscopic area of the electrode, γ is a geometrical factor, C_o^* is the constant bulk concentration, F is Faraday's constant, Γ is the gamma function, λ_i is the length corresponding to the inner cut-off of the fractal electrode, v is the scan rate, D_R is the diffusion coefficient, and i_{peak} is the maximum cathodic current (the peak current). In the case of the reversible chemical equations, the maximum cathodic current is equal to the maximum anodic current but with an opposite sign. Equation (5) is deduced taking account of the diffusion-controlled process to a fractal surface, the fractal Cottrell coefficient, and extended the Bard and Faulkner derivation for smooth electrodes to fractal surfaces [1].

The slope of the log-log plot of peak current i_{peak} versus scan rate v from Equation (5) is the fractal parameter α, which leads to the CV-fractal dimension of the fractal electrode surface: $i_{peak} \sim v^\alpha$

The macroscopic and the microscopic areas of the electrode obey the following relation [14,15]:

$$\frac{A_{macro}}{A_{micro}} = \left(\frac{\lambda_i}{\lambda_o}\right)^{2\alpha-1} \quad (6)$$

with λ_i and λ_o being the spatial inner and outer cut-offs of the fractal electrode, corresponding to the spatial self-similarity limits, related to the fastest and the slowest scan, respectively. The fastest scan will provide the inner cut-off; meanwhile, the slowest scan will provide the outer cut-off, respectively.

Equation (6) corroborated with Fick's first law of diffusion for computing inner and outer cut-offs and with fractal Randles–Sevcik equation Equation (5) lead to the following [39]:

$$\frac{A_{macro}}{A_{micro}} = \left(\frac{i_1 v_2}{i_2 v_1}\right)^{D-2} \quad (7)$$

For a fractal electrode, the active surface of the electrode is the microscopic area, which is greater than the geometric surface, described by the macroscopic area [39]. The active surface area is equal to the geometric area only in the case of a planar surface, $D = 2$ in the Euclidean space. According to Equation (6), the active surface area increases, either increasing the fractal dimension or increasing the self-similarity limits. In other words, electrodes with broader self-similarity domains and higher fractal dimensions will have a higher active surface area and, in consequence, a higher electrochemical response.

3. Results and Discussion

3.1. SEM Fractal Dimensions

SEM micrographs of the carbon paste electrode, IL/carbon paste electrode, $AuTiO_2$/GO/carbon paste electrode, and IL/$AuTiO_2$/GO/carbon paste electrode are presented in Figure 1. For every electrode, a set of SEM images at different magnitudes were collected, and after that, these images were analyzed using fractal theory. Results are presented in Tables 1–4 (Figures S1 and S2). Mean roughness was also computed using Gwyddion Data Analysis Software version 2.65 [40].

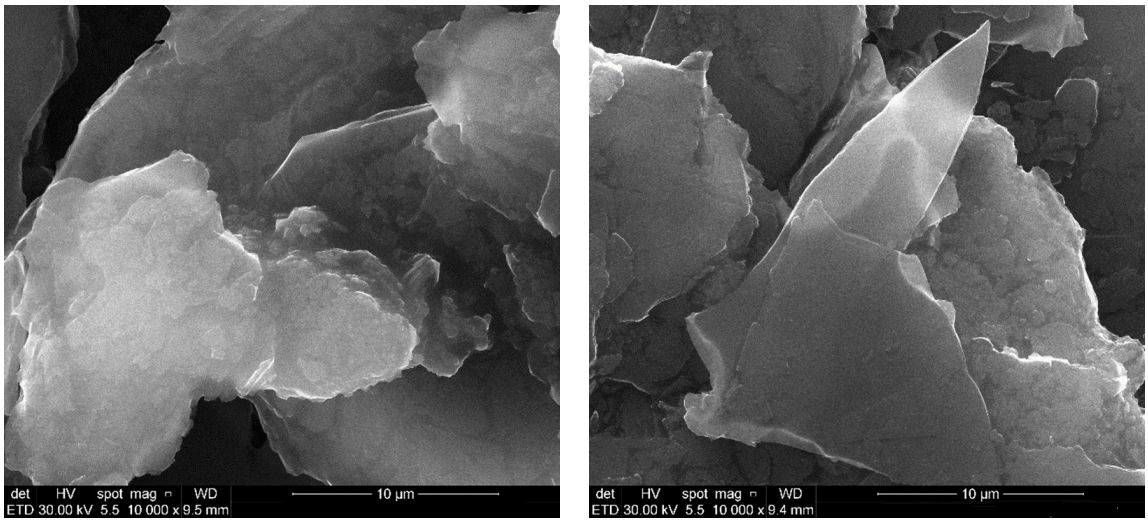

(**a**) (**b**)

Figure 1. *Cont.*

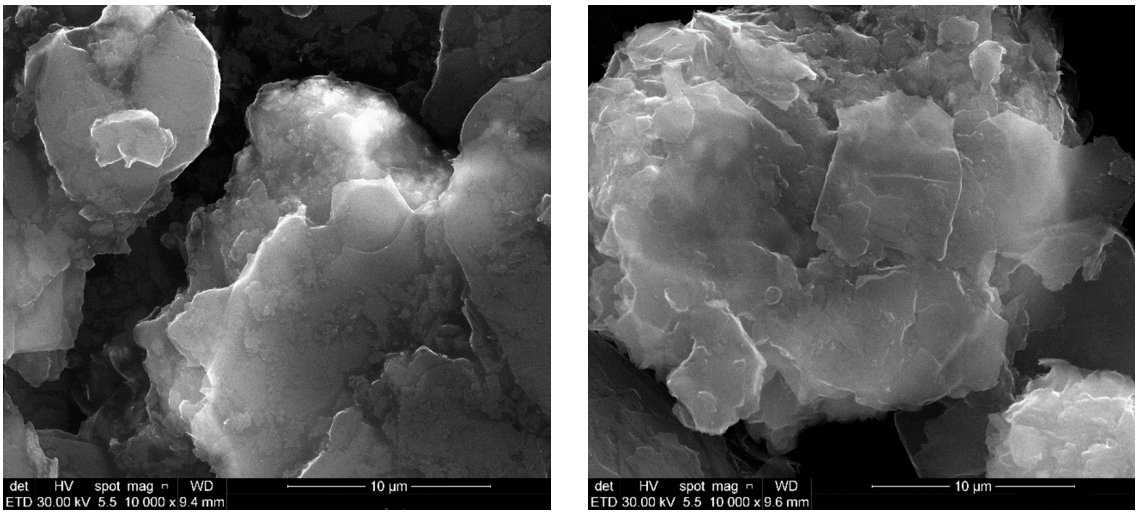

(**c**) (**d**)

Figure 1. SEM micrographs of (**a**) CPE; (**b**) IL/CPE; (**c**) $AuTiO_2$/GO/CPE; (**d**) IL/$AuTiO_2$/GO/CPE.

Table 1. Fractal dimension of carbon paste electrode (CPE).

Magnitude	Method	Fractal Dimension	Standard Errors	Determination Coefficient	Self-Similarity Domain (nm)	Mean Roughness
300 µm	Correlation Function Method	2.730	0.001	0.995	263–6595	0.1534
	Variable Length Scale Method	2.714	0.004	0.998	2636–34,270	
10 µm	Correlation Function Method	2.767	0.001	0.996	100–1186	0.1492
	Variable Length Scale Method	2.735	0.006	0.972	132–5828	
500 nm	Correlation Function Method	2.622	0.002	0.950	9–36	0.1214
	Variable Length Scale Method	2.717 2.551	0.019 0.005	0.982 0.998	13–46 46–132	

Table 2. SEM Fractal dimension of IL/carbon paste electrode (IL/CPE).

Magnitude	Method	Fractal Dimension	Standard Errors	Determination Coefficient	Self-Similarity Domain (nm)	Mean Roughness
300 µm	Correlation Function Method	2.652 2.732	0.007 0.002	0.996 0.997	264–1321 1321–3756	0.1284
	Variable Length Scale Method	2.661 2.829	0.007 0.004	0.998 0.993	2643–18,502 18,502–44,934	
10 µm	Correlation Function Method	2.779	0.001	0.997	13–2747	0.1347
	Variable Length Scale Method	2.762	0.006	0.980	132–4105	
500 nm	Correlation Function Method	2.799	0.011	0.984	2–4 (narrow self-similarity domain)	0.1136
	Variable Length Scale Method	2.788	0.018	0.956	11–88	

Table 3. SEM Fractal dimension of $AuTiO_2$/GO-modified carbon paste electrode ($AuTiO_2$/GO/CPE).

Magnitude	Method	Fractal Dimension	Standard Errors	Determination Coefficient	Self-Similarity Domain (nm)	Mean Roughness
300 µm	Correlation Function Method	2.711 2.541	0.013 0.001	0.994 0.999	264–747 747–2759	0.1516
	Variable Length Scale Method	2.520 2.781	0.010 0.015	0.998 0.973	2643–13,215 13,215–31,718	
10 µm	Correlation Function Method	2.700	0.001	0.999	13–723	0.1689
	Variable Length Scale Method	2.714 2.583	0.011 0.009	0.994 0.992	132–794 794–3178	
1 µm	Correlation Function Method	2.594	0.002	0.995	4–27	0.1696
	Variable Length Scale Method	2.576	0.004	0.995	39–529	

Table 4. SEM Fractal dimension of IL/$AuTiO_2$/GO-modified carbon paste electrode (IL/$AuTiO_2$/GO/CPE).

Magnitude	Method	Fractal Dimension	Standard Errors	Determination Coefficient	Self-Similarity Domain (nm)	Mean Roughness
300 µm	Correlation Function Method	2.767 2.600	0.011 0.002	0.982 0.989	264–953 953–2847	0.1778
	Variable Length Scale Method	2.589 2.737	0.006 0.011	0.999 0.991	5286–18,502 18,502–34,361	
10 µm	Correlation Function Method	2.749	0.001	0.998	13–2070	0.1814
	Variable Length Scale Method	2.689	0.005	0.993	261–3660	
3 µm	Correlation Function Method	2.770 2.553	0.018 0.001	0.980 0.999	2–7 7–30	0.1706
	Variable Length Scale Method	2.584	0.004	0.998	52–634	

Carbon paste electrodes exhibit fractal behavior over a large self-similarity domain, characterized by a global fractal dimension of 2.714–2.767 and a lower fractal dimension of 2.551–2.622 for lower scales. The fractal behavior over a large-scale domain indicates long-range correlations and organized structures (Table 1).

IL/CPE electrodes exhibit fractal behavior over a large self-similarity domain characterized by higher values of the fractal dimension of 2.762–2.829. The 10 µm and 500 nm samples are very well correlated, characterized by a single fractal structure (fractal dimension 2.762–2.799). The 300 µm sample (the large micrograph) has a bi-modal behavior, with a global fractal dimension of 2.829 for the high values of cut-off limits and a second fractal dimension of 2.652–2.732 for the self-similarity domain of 264 nm–18,502 nm (Table 2).

The added ionic liquid improved the fractal behavior and extended the self-similarity domain to higher cut-off limits. Comparing results presented in Tables 1 and 2, one can notice that the fractal dimension at the higher outer self-similarity limit is higher when IL is added (2.829), and the higher outer self-similarity limit is extended toward 44,934 nm, compared to 34,270 nm. Additionally, the IL/CPE electrode is characterized by higher

fractal dimensions than the initial CPE electrode (Table 2). This observation could be of interest in studying the electrochemical response of the electrode, as higher fractal dimensions will lead to higher electrochemical response [14,15,19,23]. Although there are reports of the effect of ionic liquid on fractal properties in other systems, as the fractal dimension increases when ionic liquid is added [41], more studies are required for a deeper understanding of the phenomena.

The $AuTiO_2$/GO-modified carbon paste electrode is characterized by an accentuated bi-modal fractal behavior indicating two superposed fractal structures: a structure with a lower fractal dimension of 2.520–2.594 and another one with a higher fractal dimension, a compact structure, characterized by 2.700–2.781. As the presence on the surface of $AuTiO_2$/GO was proved by SEM-EDAX characterization [1] we presume that the structure characterized by a fractal dimension of 2.520–2.594 is due to its presence on the surface.

Additionally, the structure characterized by the low fractal dimension (2.520–2.594) could be assigned to the presence on the surface of the $AuTiO_2$/GO composite, as it appears like a fractal structure not observed for the carbon paste electrode (Table 1) or for the IL/CPE electrode (Table 2). It can be observed over a large self-similarity domain, from 4 nm to 13,215 nm (Table 3); meanwhile, the lower fractal dimension structure of 2.551–2.622 (Table 1) of the carbon paste electrode is observed only for lower scales. More studies are required to fully understand the effect.

IL/$AuTiO_2$/GO electrodes exhibit two superposed fractal structures, both with strong self-similarity domains, characterized by a medium fractal dimension of 2.553–2.600 and the other one, by a higher fractal dimension of 2.689–2.770. Samples are characterized by large self-similarity domains, long-range correlations, and impressive fractal behavior. As we already noticed in the case of IL/CPE (Table 2), adding ionic liquid leads to broader self-similarity domains and higher fractal dimensions. The large self-similarity domain makes the IL/$AuTiO_2$/GO-modified carbon paste electrode an important candidate to be used as a high-quality electrode. (Table 4)

Mean roughness increases slightly with the modification of the electrodes, except for the case of IL modification, as can be seen in Tables 1–4.

3.2. Fractal Dimensions Obtained from Cyclic Voltammetry (CV-Fractal Dimensions)

Cyclic voltammetry was used to compute the fractal dimensions of electrodes and compare them with those obtained from SEM measurements. Additionally, cyclic voltammetry was used to characterize the electrochemical response of the electrodes. The scaling relation $i_{peak} \sim v^{\alpha}$ from Equation (5) in a log-log diagram leads to the fractal parameter α, and therefore, the fractal dimension D is computed. The absolute value of the maximum cathodic current (the peak current) at different scan rates is extracted from cyclic voltammograms depicted in Figure 2 (working conditions: potential range from −0.6 V to1.0 V; step potential 0.025 V; absolute temperature 298.15 K).

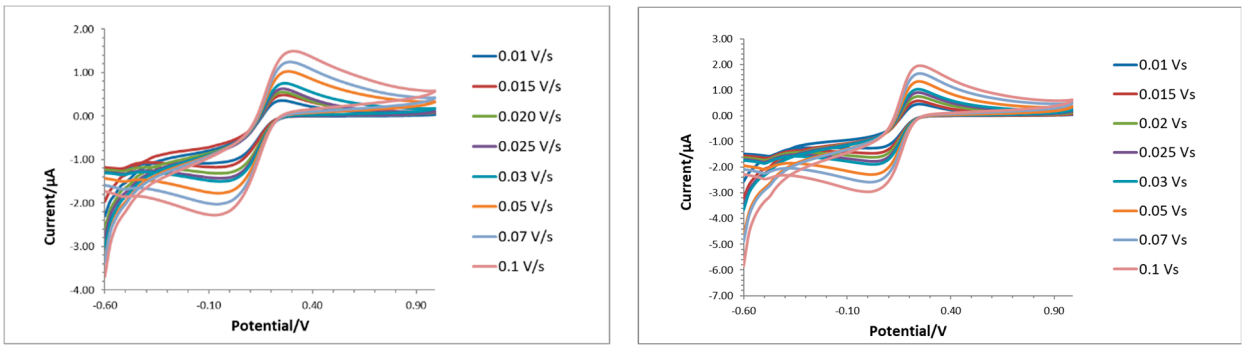

(**a**) (**b**)

Figure 2. *Cont.*

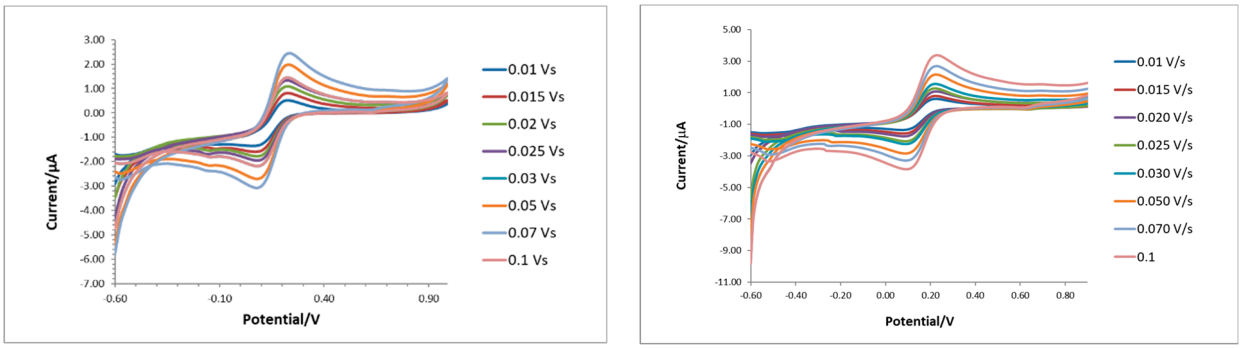

(**c**) (**d**)

Figure 2. Cyclic voltammograms in a solution of 5.0×10^{-3} mol L^{-1} $K_3[Fe(CN)_6]$ in 0.1 mol L^{-1} KCl at different scans rates from 0.010 to 0.100 V s^{-1} (**a**) CPE; (**b**) IL/CPE; (**c**) $AuTiO_2$/GO/CPE; (**d**) IL/$AuTiO_2$/GO/CPE.

The log-log diagrams of peak currents versus scan rates are presented for every electrode in Figure S3. Results obtained from line slopes are presented in Table 5.

Table 5. Cyclic voltammetry fractal dimension (CV fractal dimension) obtained from log-log plot of i_{peak} versus scan rate ν (Figure S3) (Equation (5)).

Sample	CV Fractal Dimension	Standard Errors	Determination Coefficient	Self-Similarity domain Scan Rates (V/s)
CPE	2.250	0.015	0.9964	0.01–0.1
IL/CPE	2.301	0.026	0.9903	0.01–0.1
$AuTiO_2$/GO/CPE	2.386	0.040	0.9871	0.015–0.07
IL/$AuTiO_2$/GO/CPE	2.519	0.024	0.9940	0.01–0.1

Although modifying the carbon paste electrode with $AuTiO_2$/GO composite increases the fractal dimension, at a higher scan rate, auto similarity is lost, and self-similarity properties are damaged. Table 5 shows that the self-similarity domain is restrained to 0.015–0.07. However, by adding ionic liquid, the fractal properties are enhanced, the self-similarity domain is re-established, and the fractal dimension increases again; this behavior is in good agreement with the geometric fractal dimensions obtained from SEM images (Table 4).

The IL/$AuTiO_2$/GO/CPE electrode exhibits good fractal properties and higher fractal dimension—as cyclic voltammograms depicted—than CPE, IL/CPE, and $AuTiO_2$/GO/CPE.

The fractal dimension values sequence is $D_{IL/AuTiO2/GO/CPE} > D_{AuTiO2/GO/CPE} > D_{IL/CPE} > D_{CPE}$, meaning that the IL/$AuTiO_2$/GO/CPE electrode has the highest fractal dimension, gives the highest electrochemical response [23], and it is suitable to be utilized as sensor, as it was already proven [1] for the detection of tartrazine.

The sequence is identical to the increase in the sensor conductivity (Figure 3), indicating that the modification improves electrochemical response due to geometrical self-similarity and higher fractal dimensions as a result of modifying the carbon paste electrodes with IL, $AuTiO_2$/GO, and IL/$AuTiO_2$/GO, respectively. Results are in good agreement with the EIS and CV methods [1]. Comparing the four electrodes, the IL/$AuTiO_2$/GO/CPE gave the best results for the oxidation of tartrazine. An explanation of this behavior is that higher fractal dimensions lead to higher active surfaces. These results suggest that the IL/$AuTiO_2$/GO-modified carbon paste electrode can be useful as a sensor in various analyses, not only as a Tz sensor.

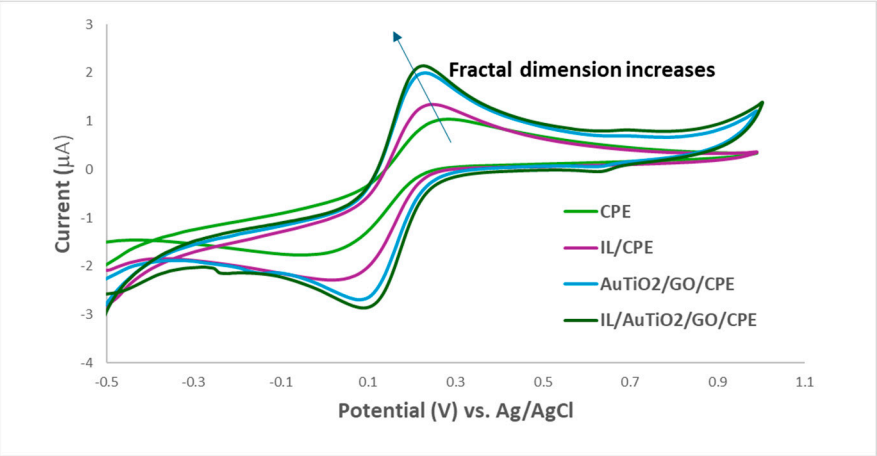

Figure 3. Cyclic voltammograms performed in a solution of 5.0×10^{-3} mol L^{-1} $K_3[Fe(CN)_6]$ (0.1 mol L^{-1} KCl); step potential 0.025 V; scan rate 0.05 V/s, using as working electrodes the CPE, IL/CPE, $AuTiO_2$/GO/CPE, and IL/$AuTiO_2$/GO/CPE.

Comparing geometric fractal dimensions obtained by SEM analysis with fractal dimensions from cyclic voltammetry, SEM fractal dimensions provide information about the "visible" geometric surface, meanwhile cyclic voltammetry offers information about active sites implied in chemical reactions (Table 6).

Table 6. Comparison between SEM fractal dimension and CV fractal dimension.

Sample	Low-Scale SEM Fractal Dimension	High-Scale SEM Fractal Dimension	CV Fractal Dimension
CPE	2.551–2.622	2.714–2.767	2.250
IL/CPE	2.779–2.799	2.829	2.301
$AuTiO_2$/GO/CPE	2.520–2.594	2.781	2.386
IL/$AuTiO_2$/GO/CPE	2.553–2.689 2.767–2.770	2.589 2.737	2.519

Although SEM fractal dimensions seem not to follow the same tendency as CV fractal dimensions, SEM fractal analysis shows that the IL/$AuTiO_2$/GO/CPE is self-similar over large scales; it is more organized than the other electrodes and has higher fractal dimensions values at low scales than the CPE electrode and $AuTiO_2$/GO/CPE electrode. Mean roughness increases in the same manner as CV fractal dimension, except for the case of the IL/carbon paste electrode.

The IL/CPE electrode is characterized by multiple fractal dimensions extended on a broad domain (2.661–2.829). However, this electrode is not the best one for the oxidation of tartrazine, meaning that the higher SEM fractal dimensions are not the major factor that influences its electrochemical features.

The differences between the two fractal dimensions (SEM and CV) occur from the hypothesis that leads to the CV fractal dimension and fractal Randles–Sevcik equation [19]. The CV fractal dimension characterizes the surface concentration of the active species on the fractal surface, and it is related both to the surface geometrical fractal dimension and to the chemical properties of the active species; the CV fractal dimension is related to the active surface and not only to the geometrical one.

Additionally, it is possible that the differences between the SEM fractal dimension and CV fractal dimension are related to the different self-similarity scales; SEM analysis is suitable for the macroscopic area, and the CV technique describes the microscopic active area [14,15,19,23,42,43]; the limits of self-similarity domain of SEM fractal dimension are larger enough to consider SEM fractal dimension as a macroscopic fractal dimension.

Stromme et al. [19] and Parveen et al. [23] proved that peak current increases with fractal dimension. The recorded cyclic voltammograms indicate that fractal dimension increases as in the sequence: $D_{IL/AuTiO2/GO/CPE} > D_{AuTiO2/GO/CPE} > D_{IL/CPE} > D_{CPE}$ and the peak current increases in the same manner (Figure 3).

Peak current depends not only on fractal dimension but also on the finest feature of fractal roughness (the inner cut-off limit) [23] and on the proportionality factor [23]. The computed SEM fractal dimensions have shown that lower inner cut-off limits correspond to higher anodic peak current, as was predicted in the literature [23].

Comparing the four electrodes, the electrode with the highest response in the anodic current is IL/$AuTiO_2$/GO/CPE; thus, it was chosen for the oxidation of tartrazine [1].

Some important remarks are to be made. Every fractal determination method is related to the physical phenomena behind it; therefore, it is not an unusual situation that two fractal dimensions computed from different methods give different results. The SEM fractal dimension of the electrode is higher than the CV fractal dimension from the cyclic voltammetry of the electrode in ferricyanide. The CV fractal dimension is a measure not only of the surface geometry but is a measure of the number of active sites on the surface. A higher fractal dimension means a higher number of active sites and higher activity.

From CV measurements, it is easy to compute the active surface area of the electrode [39] (Table 7).

Table 7. Active surface area A_{micro} computed from Equation (7).

Sample	CV Fractal Dimension	Macroscopic Area (cm^2) A_{macro}	A_{macro}/A_{micro}	Active Surface Area (cm^2)
CPE	2.250	0.0015	0.8045	0.0019
IL/CPE	2.301	0.0019	0.7809	0.0024
$AuTiO_2$/GO/CPE	2.386	0.0030	0.8442	0.0036
IL/$AuTiO_2$/GO/CPE	2.519	0.0036	0.7444	0.0048

According to results published in the literature [14,15,19,39], the active surface area of the electrode can be computed in a simple way from cyclic voltammetry data. Only the peak currents and the scan rates corresponding to the inner and outer cut-offs, meaning the fastest scan rate and the slowest scan rate, respectively, are necessary to compute the active surface of the electrode—the microscopic area (Equation (7)).

The following table presents results computed using the method described in previous cited works [14,15,19,39]. The macroscopic area was computed in previous published work [1]; Equation (7) was used to compute the microscopic area, with i_1, υ_1 being the peak current and the scan rate of the fastest scan corresponding to the inner cut-off and i_2, υ_2 being the peak current and the scan rate of the slowest scan corresponding to the outer cut-off.

It is important to notice that a high self-similarity domain means higher ν_1/ν_2 ratios, leading to higher A_{micro}/A_{macro} ratios and higher electrode active area. The conclusion is straightforward: a method to increase electrode active area is to improve the domain of self-similarity, not only to increase the fractal dimension.

Therefore, to obtain materials with high electrochemical response and to use them as sensors, there are two possible directions to follow: to obtain materials with high fractal dimensions and/or to obtain materials with higher self-similarity domains, meaning that materials with higher fractal dimensions and fractal properties over large scales are characterized by higher active areas and higher electrochemical activity.

The electrode with the best electrochemical properties and the best fractal behavior was proven to be IL/$AuTiO_2$/GO/CPE, which recommended it as a sensor for the detection of Tz in real food samples, as was already proven [1].

The carbon paste electrodes turn out to be useful materials in electrochemical research. They are easy to modify, show low background current, low resistance, and low cost. In the context of finding materials suitable to be used as electrochemical sensors, electrode characterization is an important step for sensor design. Looking for materials with higher fractal dimensions and broader self-similarity domains are two priority research directions for tailoring higher-sensitivity sensors.

4. Conclusions

This paper investigated the fractal properties of four different carbon paste electrodes: CPE, IL/CPE, $AuTiO_2$/GO/CPE, and IL/$AuTIO_2$/GO/CPE. The electrodes' fractal dimensions were computed using two different techniques: image analysis of SEM micrographs (SEM fractal dimension) and cyclic-voltammograms analysis (CV fractal dimension). SEM fractal dimension and CV fractal dimension were compared with each other. Meanwhile, SEM fractal dimensions are related to geometrical surface properties, and CV fractal dimensions offer information about the active surface. The cyclic voltammogram technique led to the computation of both fractal dimension and active surface area. The fractal properties of the electrodes were compared to their electrochemical responses, indicating good correlations between the intensity of the peak current and fractal dimension and between the self-similarity domain and the active surface area (the microscopic area). The electrode that proved to have the best fractal behavior, both in terms of higher fractal dimensions and higher self-similarity domain, the highest active surface, and the highest electrochemical response was IL/$AuTiO_2$/GO/CPE, which is also the best sensor for the detection of Tz in real food samples [1]. A major conclusion of this work is that to design electrodes with high electrochemical response, both the fractal dimension and self-similarity domain must be high; more studies are to be done in this research direction.

Supplementary Materials: The following supporting information can be downloaded at: https://www.mdpi.com/article/10.3390/fractalfract8040205/s1, Figure S1. Log-log graph of correlation function versus squared radius for IL/$AuTiO_2$/GO modified carbon paste electrode, Figure S2. Log-log graph of rms deviation function versus box-size ε for IL/$AuTiO_2$/GO modified carbon paste electrode, Figure S3. Log-log diagrams of peak current versus scan rate in the self-similarity regime; the slope of the curve gives the fractal parameter α and, therefore, the fractal dimension D = 2α + 1; (a) CPE; (b) IL/CPE; (c) $AuTiO_2$/GO/CPE; (d) IL/$AuTiO_2$/GO/CPE.

Author Contributions: Conceptualization, G.D., F.P. and R.N.S.; methodology, G.D.; validation, G.D., F.P. and R.N.S.; formal analysis, G.D.; investigation, G.D., F.P., R.G.-S. and R.N.S.; resources, R.G.-S. and R.N.S.; data curation, R.G.-S. and R.N.S.; writing—original draft preparation, G.D., F.P. and R.N.S.; writing—review and editing, G.D., F.P., R.G.-S., J.F.v.S. and R.N.S. All authors have read and agreed to the published version of the manuscript.

Funding: This research received no external funding.

Data Availability Statement: Data are contained within the article and Supplementary Materials.

Conflicts of Interest: The authors declare no conflicts of interest.

References

1. Georgescu State, R.; van Staden, J.K.; State, R.N.; Papa, F. Rapid and sensitive electrochemical determination of tartrazine in commercial food samples using IL/$AuTiO_2$/GO composite modified carbon paste electrode. *Food Chem.* **2022**, *385*, 132616–132625. [CrossRef]
2. Zhao, L.; Zeng, B.; Zhao, F. Electrochemical determination of tartrazine using a molecularly imprinted polymer—Multiwalled carbon nanotubes—Ionic liquid supported Pt nanoparticles composite film coated electrode. *Electrochim. Acta* **2014**, *146*, 611–617. [CrossRef]
3. Zhao, X.; Liu, Y.; Zuo, J.; Zhang, J.; Zhu, L.; Zhang, J. Rapid and sensitive determination of tartrazine using a molecularly imprinted copolymer modified carbon electrode (MIP-PmDB/PoPD-GCE). *J. Electroanal. Chem.* **2017**, *785*, 90–95. [CrossRef]
4. Chikere, C.O.; Hobben, E.; Faisal, N.H.; Kong-Thoo-Lin, P.; Fernandez, C. Electroanalytical determination of gallic acid in red and white wine samples using cobalt oxide nanoparticles-modified carbon-paste electrodes. *Microchem. J.* **2021**, *160*, 105668–105672. [CrossRef]

5. Hernandez-Vargas, S.G.; Alberto Cevallos-Morillo, C.; Aguilar-Cordero, J.C. Effect of ionic liquid structure on the electrochemical response of dopamine at room temperature ionic liquid-modified carbon paste electrodes (IL–CPE). *Electroanalysis* **2020**, *32*, 1938–1948. [CrossRef]
6. Mandelbrot, B.B. *The Fractal Geometry of Nature*; W. H. Freeman and Company: San Francisco, CA, USA, 1982.
7. Avnir, D.; Farin, D.; Pfeifer, P. Surface geometric irregularity of particulate materials: The fractal approach. *J. Colloid. Interface Sci.* **1985**, *103*, 112–123. [CrossRef]
8. Rothschild, W.G. Fractals in heterogeneous catalysis. *Catal. Rev. Sci. Eng.* **1991**, *33*, 71–107. [CrossRef]
9. Dobrescu, G.; Papa, F.; State, R.; Raciulete, M.; Berger, D.; Balint, I.; Ionescu, N.I. Modified Catalysts and Their Fractal Properties. *Catalysts* **2021**, *11*, 1518–1533. [CrossRef]
10. Pfeifer, P.; Johnston, G.P.; Deshpande, R.; Smith, D.M.; Hurd, A.J. Structure analysis of porous solids from preadsorbed films. *Langmuir* **1991**, *7*, 2833–2843. [CrossRef]
11. Gutfraind, R.; Sheintuch, M.; Avnir, D. Fractal and multifractal analysis of the sensitivity of catalytic reactions to catalyst structure. *J. Chem. Phys.* **1991**, *95*, 6100–6111. [CrossRef]
12. Petcu, G.; Dobrescu, G.; Blin, J.-L.; Atkinson, I.; Ciobanu, M.; Parvulescu, V. Evolution of morphology, fractal dimensions and structure of (titanium) aluminosilicate gel during synthesis of zeolites Y and Ti-Y. *Fractal Fract.* **2022**, *6*, 663–674. [CrossRef]
13. Park, B.Y.; Zaouk, R.; Wang, C.; Madou, M.J. A Case for Fractal Electrodes in Electrochemical Applications. *J. Electrochem. Soc.* **2007**, *154*, P1–P5. [CrossRef]
14. Pajkossy, T.; Nyikos, L. Diffusion to fractal surfaces—II. Verification of theory. *Electrochem. Acta* **1989**, *34*, 171–179. [CrossRef]
15. Pajkossy, T.; Nyikos, L. Diffusion to fractal surfaces—III. Linear sweep and cyclic voltammograms. *Electrochim. Acta* **1989**, *34*, 181–186. [CrossRef]
16. Mahjani, M.G.; Moshrefi, R.; Sharifi-Viand, A.; Taherzad, A.; Jafarian, M.; Hasanlou, F.; Hosseini, M. Surface investigation by electrochemical methods and application of chaos theory and fractal geometry. *Chaos Solitons Fract.* **2016**, *91*, 598–603. [CrossRef]
17. Eftekhari, A. Fractal dimension of electrochemical reactions. *J. Electrochem. Soc.* **2004**, *151*, E291–E297. [CrossRef]
18. Molaei, F.; Eftekhari, A. Fractal Analysis by Means of Electrochemical Methods: The Usefulness of Gold-Masking Approach. In *ECS Meeting Abstracts*; IOP Publishing: Bristol, UK, 2006; p. 1865.
19. Stromme, M.; Niklasson, G.A.; Granqvist, C.G. Voltammetry on fractals. *Solid. State Commun.* **1995**, *96*, 151–154. [CrossRef]
20. Dobrescu, G.; Papa, F.; State, R.; Balint, I. Characterization of bimetallic nanoparticles by fractal analysis. *Powder Technol.* **2018**, *338*, 905–914. [CrossRef]
21. State, R.; Papa, F.; Dobrescu, G.; Munteanu, C.; Atkinson, I.; Balint, I. Green synthesis and characterization of gold nanoparticles obtained by a direct reduction method and their fractal dimension. *Environ. Eng. Manag. J.* **2015**, *14*, 587–593. [CrossRef]
22. Eftekhari, A. Electrochemical technique for the determination of fractal dimension of dental surfaces. *Colloids Surf. B Biointerfaces* **2003**, *32*, 375–381. [CrossRef]
23. Parveen, R.K. Theory for staircase voltammetry and linear voltammetry on fractal electrodes: Emergence of anomalous Randles-Sevcik behavior. *Electrochim. Acta* **2013**, *111*, 223–233. [CrossRef]
24. Andrieux, C.P.; Audebert, P. Electron Transfer through a Modified Electrode with a Fractal Structure: Cyclic Voltammetry and Chronoamperometry Responses. *J. Phys. Chem. B* **2001**, *105*, 444–448. [CrossRef]
25. Tence, M.; Chevalier, J.P.; Jullien, R. On the measurement of the fractal dimension of aggregated particles by electron microscopy: Experimental method, corrections and comparison with numerical models. *J. Phys.* **1986**, *47*, 1989–1998. [CrossRef]
26. Teixeira, J. Small-Angle Scattering by Fractal Systems. *J. Appl. Cryst.* **1988**, *21*, 781–785. [CrossRef]
27. Bale, H.D.; Schmidt, P.W. Small-Angle X-Ray-Scattering Investigation of Submicroscopic Porosity with Fractal Properties. *Phys. Rev. Lett.* **1984**, *53*, 596–599. [CrossRef]
28. Keefer, K.D.; Schaefer, D.W. Growth of Fractally Rough Colloids. *Phys. Rev. Lett.* **1986**, *56*, 2376–2379. [CrossRef] [PubMed]
29. Schmidt, P.W. Small-angle scattering studies of disordered, porous and fractal systems. *J. Appl. Cryst.* **1991**, *24*, 414–435. [CrossRef]
30. Avnir, D.; Jaroniec, M. An isotherm equation for adsorption on fractal surfaces of heterogeneous porous materials. *Langmuir* **1989**, *5*, 1431–1433. [CrossRef]
31. Fripiat, I.J.; Gatineau, L.; van Damme, H. Multilayer physical adsorption on fractal surfaces. *Langmuir* **1986**, *2*, 562–567. [CrossRef]
32. Pfeifer, P.; Wu, Y.J.; Cole, M.W.; Krim, J. Multilayer adsorption on a fractally rough surface. *Phys. Rev. Lett.* **1989**, *62*, 1997–2000. [CrossRef]
33. Kaneko, K.; Sato, M.; Suzuki, T.; Fujiwara, Y.; Nishikawa, K.; Jaroniec, M. Surface fractal dimension of microporous carbon fibres by nitrogen adsorption. *J. Chem. Soc. Faraday Trans.* **1991**, *87*, 179–184. [CrossRef]
34. Papa, F.; Negrila, C.; Miyazaki, A.; Balint, I. Morphology and chemical state of PVP-protected Pt, Pt–Cu, and Pt–Ag nanoparticles prepared by alkaline polyol method. *J. Nanoparticle Res.* **2011**, *13*, 5057–5064. [CrossRef]
35. Schepers, H.E.; van Beek, J.H.G.M.; Bassingthwaighte, J.B. Four methods to estimate the fractal dimension from self-affine signals (medical application). *IEEE Eng. Med. Biol.* **1992**, *11*, 57–64. [CrossRef] [PubMed]
36. Botet, R.; Jullien, R. A theory of aggregating systems of particles: The clustering of clusters process. *Ann. Phys. Fr.* **1988**, *13*, 153–221. [CrossRef]
37. Family, F.; Vicsek, T. Scaling of the active zone in the Eden process on percolation networks and the ballistic deposition model. *J. Phys. A Math. Gen.* **1985**, *18*, L75–L81. [CrossRef]

38. Chauvy, P.F.; Madore, C.; Landolt, D. Variable length scale analysis of surface topography: Characterization of titanium surfaces for biomedical applications. *Surf. Coat. Technol.* **1998**, *110*, 48–56. [CrossRef]
39. Eftekhari, A. Calculation of the Active Surface Area of Electrodes by Means of Fractal Dimension. Available online: http://preprint.chemweb.com/physchem/0011005 (accessed on 16 November 2000).
40. Nečas, D.; Klapetek, P. Gwyddion: An open-source software for SPM data analysis. *Cent. Eur. J. Phys.* **2012**, *10*, 181–188. [CrossRef]
41. Zhao, L.; Guanhua, N.; Lulu, S.; Qian, S.; Shang, L.; Kai, D.; Jingna, X.; Gang, W. Effect of ionic liquid treatment on pore structure and fractal characteristics of low rank coal. *Fuel* **2020**, *262*, 116513. [CrossRef]
42. Pehlivan, E.; Niklasson, G.A. Fractal dimensions of niobium oxide films probed by protons and lithium ions. *J. Appl. Phys.* **2006**, *100*, 053506–053509. [CrossRef]
43. Shin, H.-C.; Pyun, S.-I. Application of Fractal Geometry to Interfacial Electrochemistry—I. Diffusion Kinetics at Fractal Electrodes. *J. Korean Electrochem. Soc.* **2001**, *4*, 21–25.

Disclaimer/Publisher's Note: The statements, opinions and data contained in all publications are solely those of the individual author(s) and contributor(s) and not of MDPI and/or the editor(s). MDPI and/or the editor(s) disclaim responsibility for any injury to people or property resulting from any ideas, methods, instructions or products referred to in the content.